

RESEARCH PAPER

Facile green synthesis and characterization of zinc oxide nanoparticles using tragacanth gel: investigation of their photocatalytic performance for dye degradation under visible light irradiation

Saeid Taghavi Fardood*, Farzaneh Moradnia, Amir Hossein Ghalaichi, Shokoofeh Daneshpajooh, Maryam Heidari

Department of Chemistry, University of Zanjan, Zanjan, Iran

ARTICLE INFO

Article History:

Received 24 October 2019

Accepted 15 January 2020

Published 15 February 2020

Keywords:

Zinc oxide

Green synthesis

Tragacanth gel

Malachite green dye

Photocatalytic activity

ABSTRACT

In this work, zinc oxide nanoparticles are synthesized via the green and easy sol-gel method. Then, they are characterized by Fourier transforms infrared spectroscopy (FTIR), powder X-ray diffraction (XRD), UV-visible diffuse reflectance spectroscopy (DRS), transmission electron microscope (TEM), field emission scanning electron microscopy (FESEM), and Brunauer Emmett Teller (BET) analysis. The XRD result showed that ZnO nanoparticles have a hexagonal phase structure with an average crystallite size of 18 nm. The TEM results revealed the nanoparticles' size of about 25-35 nm with spherical morphology. The optical Tauc-based band gap was found to be 3.03 eV. The BET analysis was performed to determine the specific surface area of the ZnO NPs, 15.87 m²/g. The impact of various parameters such as catalyst dosage, dye concentration, visible light irradiation and time were evaluated in dye degradation. The ZnO NPs showed a high photocatalytic performance for degradation of malachite green dye at room temperature in aqueous solution so that 92% of malachite green (MG) was degraded in 90 min.

How to cite this article

Taghavi Fardood S., Moradnia F., Ghalaichi AH., Daneshpajooh Sh., Heidari M. Facile green synthesis and characterization of zinc oxide nanoparticles using tragacanth gel: investigation of their photocatalytic performance for dye degradation under visible light irradiation. *Nanochem Res*, 2020; 5(1):69-76. DOI: 10.22036/ncr.2020.01.007

INTRODUCTION

Nanotechnology is the science related to the synthesis and utilization of NPs in different fields such as environment, food, health, chemistry, physics, biology, drug delivery, cosmetics, engineering, etc. [1-7]. Nanoparticles are of main attention due to their very small size and large surface to volume ratio. Also, nanomaterials exhibit effective features such as chemical steadiness, thermal conductivity, and high catalytic reactivity [8, 9]. Diverse methods have been presented for the synthesis of nanoparticles such as physical, chemical, and green methods [10-12].

Recently, researchers have focused on green synthesis methods to synthesize the metal nanoparticles with favorable size and, morphology [13-15]. Some advantages of this method are the cost-efficiency, quickness, safety and being ecological-friendly [16-20]. A green synthesis is an approach in which the NPs are produced by plants, algae, fungi, bacteria, etc. [21-24]

Water pollution is one of the important challenges of present decade, so propound a solution to wastewater treatment is particularly important. Photocatalysis has been used as the significant and impressive approach to remove the pollutants in water and wastewater [25, 26].

* Corresponding Author Email: saeidt64@gmail.com

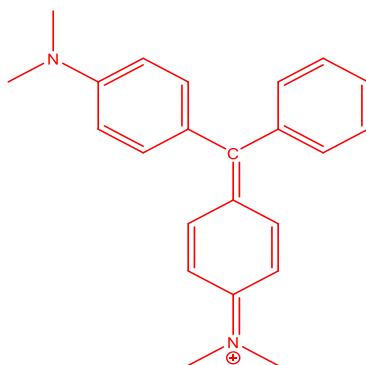


Fig. 1. Structure of malachite green (MG)

Herein, tragacanth gum is used to prepare the zinc oxide nanoparticles via green sol-gel method. The synthesized nanoparticles are applied in photocatalysis for malachite green degradation in aqueous solution under visible irradiation. ZnO NPs are characterized by FTIR, XRD, TEM, SEM, DRS, and BET. The chemical structure of malachite green dye is shown in Fig. 1.

EXPERIMENT

Materials

The tragacanth gum (TG) was purchased from a health food store. The $\text{Zn}(\text{NO}_3)_2 \cdot 6\text{H}_2\text{O}$ compound was prepared from Merck and was consumed when received. The structural properties of ZnO NPs were characterized by X-ray powder diffraction (XRD) technique on X'Pert-PRO advanced diffractometer using Cu ($K\alpha$) radiation (wavelength: 1.5406 Å) in the range of 2θ from 10 to 80. The external structure of ZnO was investigated by a Jasco 6300 Fourier transform infrared (FTIR) spectroscopy. The UV-Vis absorption spectra were prepared on a Metrohm (Analytical Jena-Specord 205) double-beam instrument. The optical properties of the synthesized zinc oxide were evaluated by UV-Vis DRS (Shimadzu, UV-2550, Japan) by using BaSO_4 as a reference. The specific surface area of the ZnO was determined by the BET nitrogen absorption/desorption technique in the Belsorp Mini II apparatus. The compound morphology and size of the sample surfaces were studied by scanning electron microscope (Zeiss EVO 18, Germany) and the TEM (Philips CM30) analysis.

Synthesis of Zinc Oxide nanoparticles

$\text{Zn}(\text{NO}_3)_2 \cdot 6\text{H}_2\text{O}$ was used as starting material for the synthesis of ZnO NPs. In the first step, 0.2 g of the tragacanth gum (TG) was added in 40 ml of

deionized water and mixed for 80 min at 70 °C. Next step, 1.5 g of zinc salt was added to the obtained gel. The container was moved to a sand bath with the stabled temperature at 75 °C and stirring was consecutive for 12 h. The product of this step was a white color resin. Then, this resin was calcined in air at 500 °C for 4 h to obtain ZnO NPs.

Photocatalytic experiment

All photocatalytic tests were done by a fluorescent lamp ($\lambda > 400$, 90 W, parmis, Iran). The degradation of the selected dye was followed in 50 ml solution of different dye concentrations. Diverse dosages of ZnO nanoparticles (0.03, 0.04, 0.05 and 0.06) were used. The degradation efficiency of malachite green dye was evaluated by UV-Vis spectrophotometer at a $\lambda_{\text{max}} = 619$ nm.

RESULTS AND DISCUSSION

Characterization of Zinc Oxide NPs

The phase and structure of the ZnO nanoparticles were determined by the XRD technique. Fig. 2 showed the XRD pattern of zinc oxide NPs. The peaks located at 31.77°, 34.39°, 36.30°, 47.53°, 56.52°, 62.91°, 66.33°, 67.82°, 69.08°, 72.45°, 76.90°, 81.33°, 89.24°, 92.62°, 95.22° and 98.65° correspond to (100), (002), (101), (102), (110), (103), (200), (112), (201), (004), (202), (104), (203), (210), (211), and (114) crystal planes of ZnO, respectively (JCPDS file No. 65-3411). All the diffraction peaks were readily indexed to a pure phase hexagonal structure. The average crystallite size of ZnO nanoparticles was obtained from the full width at half maximum (FWHM) of the (101) diffraction peak with the Scherrer formula:

$$D = \frac{0.9\lambda}{\beta \cos \theta}$$

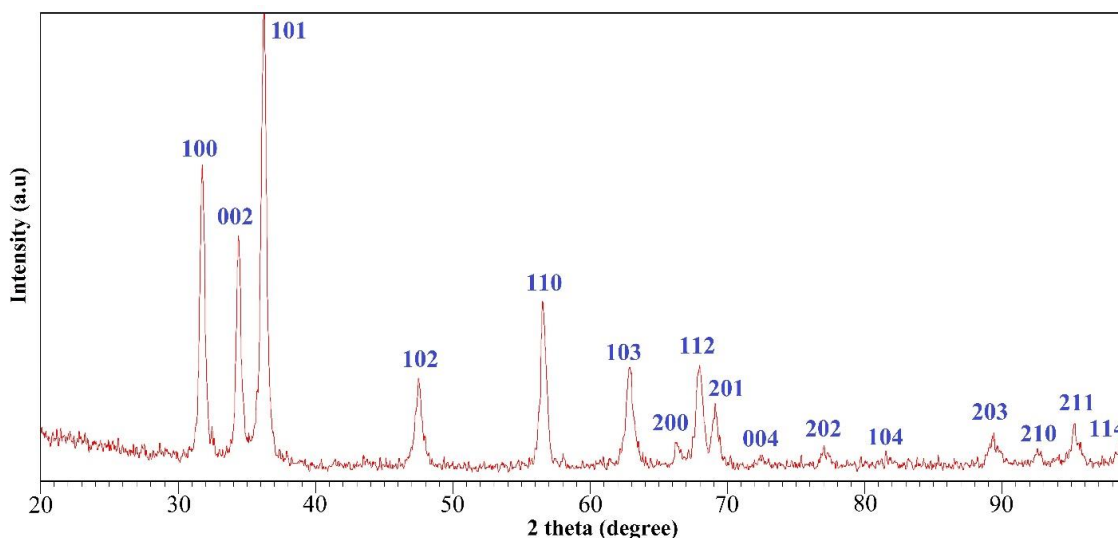


Fig. 2. XRD pattern of ZnO NPs

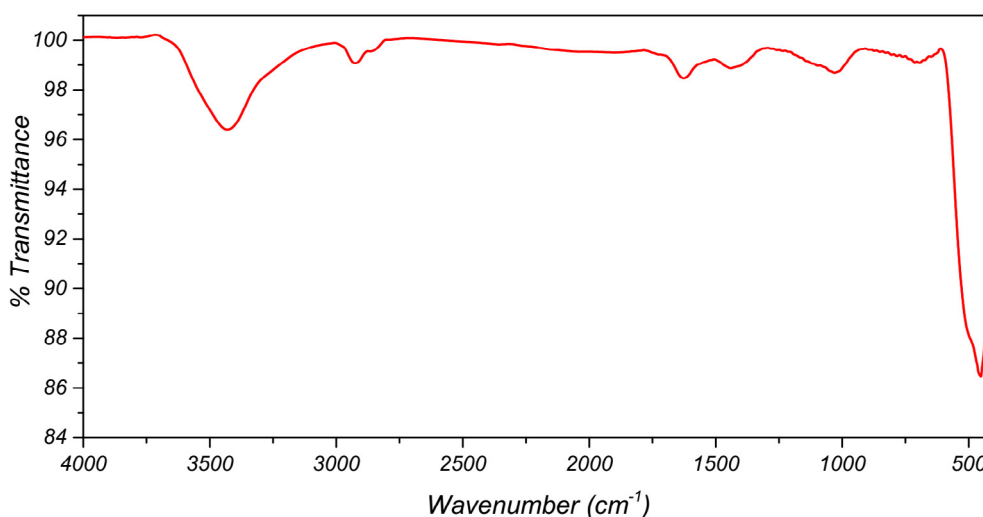


Fig. 3. FTIR spectrum of ZnO NPs.

where D is the crystallite size of the catalyst (nm), β is the full width at half maximum (FWHM) of the peak, λ is the X-ray wavelength and θ is the diffraction angle [27]. Using the above formula, we gained an average crystallite size of 18 nm for ZnO NPs.

Fig. 3 demonstrates the FTIR spectrum of zinc oxide NPs. For this sample, the bands observed at 452 cm^{-1} , 1624 cm^{-1} , and 3425 cm^{-1} are attributed to Zn–O, O–H bending, and stretching vibration of O–H group, respectively [28].

Fig. 4 displays the FESEM image of green synthesized ZnONPs. As seen in the FESEM image,

the zinc oxide NPs have narrow size distributions with uniform spherical shape. Moreover, the TEM images (Fig. 5) of the ZnO NPs were in a good agreement with the SEM image, and also showed that the prepared sample has a spherical morphology with a regular particle size of about 25–35 nm.

The specific surface area ($15.87\text{ m}^2\text{g}^{-1}$), pore diameter (45.73 nm), and total pore volume ($0.067\text{ cm}^3\text{ g}^{-1}$) of ZnO NPs were specified by the BET method.

The band gap of zinc oxide nanoparticles was evaluated by diffuse reflectance spectroscopy

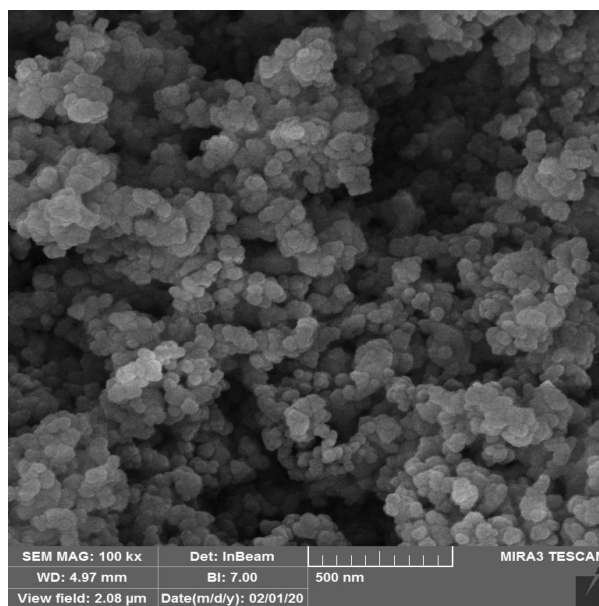


Fig. 4. SEM micrograph of the ZnO NPs.

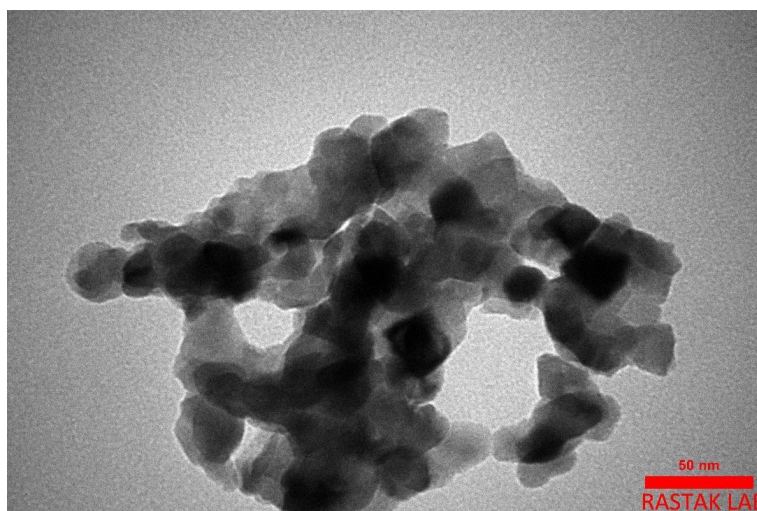


Fig. 5. TEM micrograph of the ZnO NPs.

(DRS). The band gap energy was obtained by a reflectance technique by exerting the Tauc theory [29]. The result exhibited that the band gap of ZnO nanoparticles is nearly 3.03 eV (Fig. 6). Hence, it is confirmed that the ZnO NPs are suitable photocatalyst in a visible-light region.

Effect of visible light irradiation and Zinc Oxide NPs

The photocatalytic activity of ZnO NPs on degradation Malachite Green (MG) dye was

appraised under the three states: ZnO nanoparticles under visible light irradiation (photocatalysis), Zinc oxide NPs under dark (adsorption), and visible light irradiation without ZnO NPs (photolysis). As shown in Fig. 7, the simultaneous use of ZnO NPs with visible light irradiation has led to degradation of 92 % of MG dye within 90 min. In the photolysis state, we do not have dye degradation. When the reaction was surveyed in the presence of catalyst under dark, adsorption of dye was achieved 56 %.

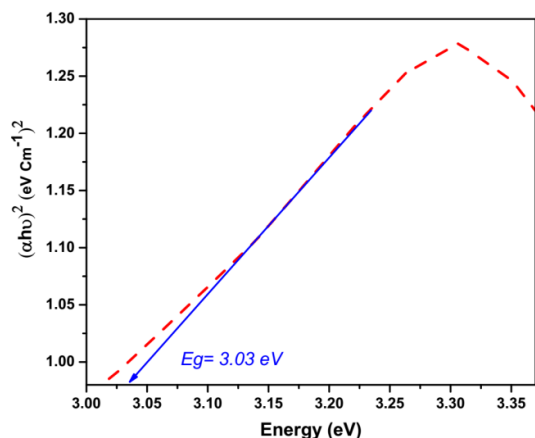


Fig. 6. Tauc plot of the ZnO NPs.

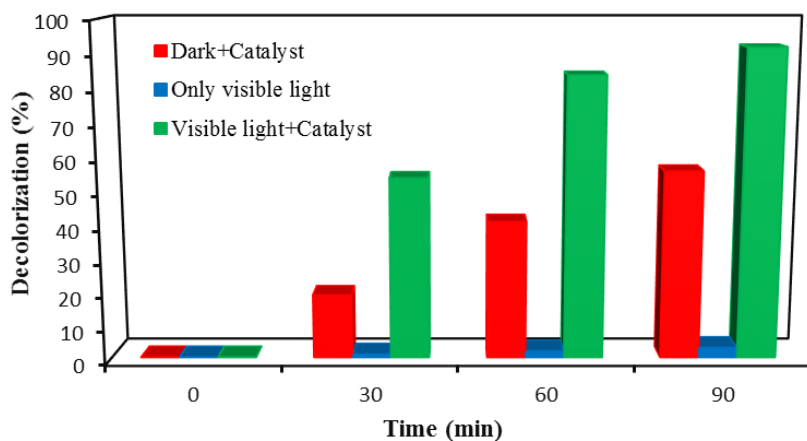


Fig. 7. Effect of visible light irradiation on the decolorization efficiency (%). Reaction conditions: MG =10 mg/L, catalyst= 0.05 g, pH=natural and room temperature

Effect of Zinc Oxide dosage

To survey the impact of the zinc oxide dosage on decolorization, different amounts of the ZnO NPs were consumed. In this test, 0.03- 0.06 g of the ZnO was used in 10 mg/L concentration of MG dye and at a constant time of 90 min. Fig. 8 displays the effect of photocatalyst dosage on dye decolorization performance for 90 min. It can be found that enhancing the catalyst amount causes to increase the removal of MG dye.

Effect of initial dye concentration

Concentration of dye is an important parameter to enhance the performance in photocatalytic dye degradation [30]. So, photocatalytic degradation of MG dye was followed by changing the initial dye concentrations (6, 8, 10, 12 mg/L) with a

constant ZnO amount (0.05 g). As presented in Fig. 9, the degradation efficiency of MG dye has been decreased from 92% to 82%, while the initial dye concentration increased from 10 to 12 mg/L.

The effect of irradiation time on the dye degradation

The UV-Vis absorption spectra of the MG dye were monitored to determine the photodegradation in the presence of zinc oxide nano photocatalyst at different irradiation times. The UV-Vis absorbance spectra were explored to demonstrate the effect of irradiation time on decolorization efficiency. The decrease in absorbance intensity at 619 nm (maximum wavelength of MG dye) with increase the irradiation time is confirmed in Fig. 10. Roughly 92% of MG was degraded in 90 min.

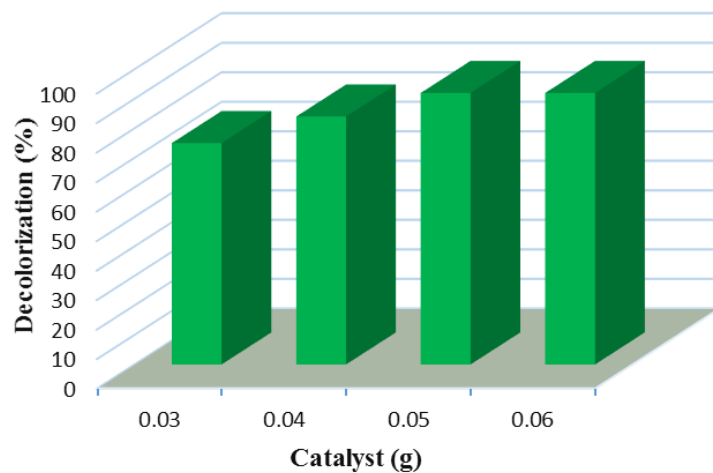


Fig. 8. The effect of photocatalyst dosage on the photocatalytic degradation of MG dye (pH = natural, MG=10 mg/L)

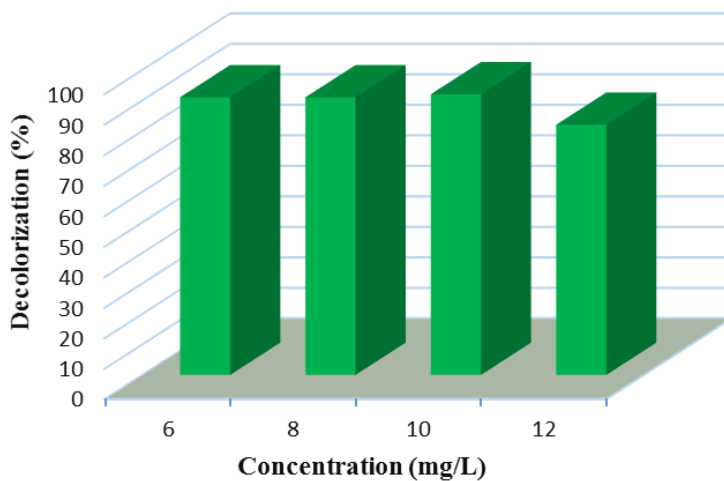


Fig. 9. The effect of the initial concentration of MG dye on the decolorization efficiency (%).

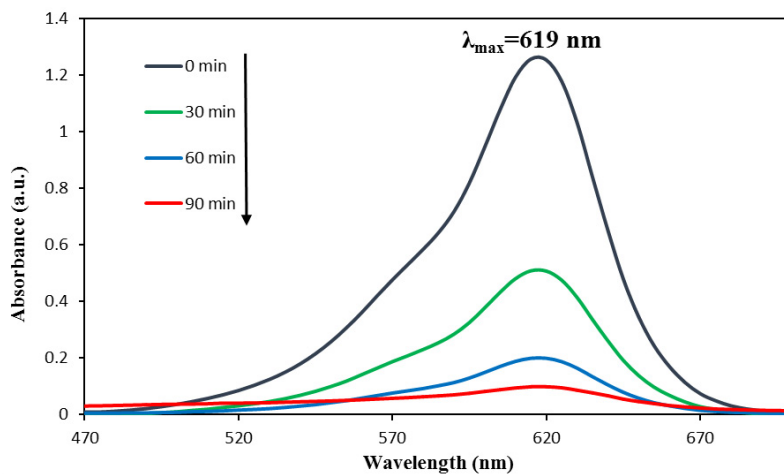


Fig. 10. Absorption spectra of MG solution (10 mg/L) in the presence of 0.05 g of ZnO photocatalyst

CONCLUSION

In this study, we present the green synthesis of ZnO NPs using tragacanth gum by the sol-gel method. This method has many benefits such as low cost, non-toxic, compounds uniform, simple work-up, and high efficiency. The synthesized nanoparticles were characterized by FTIR, XRD, TEM, SEM, DRS, and BET analyses. The photocatalytic activity of the ZnO nanoparticles was investigated for degradation of malachite green dye under visible light irradiation. The results showed that 92% of the selected dye is removed within 90 min. The effect of visible light, photocatalyst dosage, initial dye concentration, and irradiation time was surveyed separately.

ACKNOWLEDGMENT

This work was supported by the “University of Zanjan”.

CONFLICT OF INTEREST

The authors confirm that this article content has no conflict of interest.

REFERENCES

1. Singh T, Shukla S, Kumar P, Wahla V, Bajpai VK, Rather IA. Application of Nanotechnology in Food Science: Perception and Overview. *Frontiers in Microbiology*. 2017;8.
2. Nejati-Koshki K, Mortazavi Y, Pilehvar-Soltanahmadi Y, Sheoran S, Zarghami N. An update on application of nanotechnology and stem cells in spinal cord injury regeneration. *Biomedicine & Pharmacotherapy*. 2017;90:85-92.
3. He X, Deng H, Hwang H-m. The current application of nanotechnology in food and agriculture. *Journal of Food and Drug Analysis*. 2019;27(1):1-21.
4. Jahangirian H, Ghasemian lemraski E, Webster TJ, Rafiee-Moghaddam R, Abdollahi Y. A review of drug delivery systems based on nanotechnology and green chemistry: green nanomedicine. *International Journal of Nanomedicine*. 2017;Volume 12:2957-78.
5. Ali JA, Kolo K, Manshad AK, Mohammadi AH. Recent advances in application of nanotechnology in chemical enhanced oil recovery: Effects of nanoparticles on wettability alteration, interfacial tension reduction, and flooding. *Egyptian Journal of Petroleum*. 2018;27(4):1371-83.
6. Man RWY, Li C-H, MacLean MWA, Zenkina OV, Zamora MT, Saunders LN, et al. Ultrastable Gold Nanoparticles Modified by Bidentate N-Heterocyclic Carbene Ligands. *Journal of the American Chemical Society*. 2018;140(5):1576-9.
- [7] Ramazani A, Farshadi A, Mahyari A, Sadri F, Joo SW, Azimzadeh Asiabi P, et al. Synthesis of electron-poor N-Vinylimidazole derivatives catalyzed by Silica nanoparticles under solvent-free conditions. *International Journal of Nano Dimension*. 2016;7(1):41-8.
8. Ramazani A, Moradnia F, Aghahosseini H, Abdolmaleki I. Several Species of Nucleophiles in the Smiles Rearrangement. *Current Organic Chemistry*. 2017;21(16).
9. Ajormal F, Moradnia F, Taghavi Fardood S, Ramazani A. Zinc Ferrite Nanoparticles in Photo-Degradation of Dye: Mini-Review. *Journal of Chemical Reviews*. 2020;2(2):90-102.
10. Gahlawat G, Choudhury AR. A review on the biosynthesis of metal and metal salt nanoparticles by microbes. *RSC Advances*. 2019;9(23):12944-67.
11. Agarwal H, Nakara A, Shanmugam VK. Anti-inflammatory mechanism of various metal and metal oxide nanoparticles synthesized using plant extracts: A review. *Biomedicine & Pharmacotherapy*. 2019;109:2561-72.
12. Agarwal H, Venkat Kumar S, Rajeshkumar S. A review on green synthesis of zinc oxide nanoparticles – An eco-friendly approach. *Resource-Efficient Technologies*. 2017;3(4):406-13.
- [13] Taghavi Fardood S, Moradnia F, Moradi S, Foroootan R, Yekke Zare F, Heidari M. Eco-friendly synthesis and characterization of α -Fe₂O₃ nanoparticles and study of their photocatalytic activity for degradation of Congo red dye. *Nanochemistry Research*. 2019;4(2):140-7.
- [14] Naveed R, Nadeem R, Asghar M, Rahman SU, Naveed A, Ali S, et al. Ziziphus mauritiana mediated synthesis of copper and nickel nanoparticles for comparative efficacy in biological water purification. *Nanochemistry Research*. 2019;4(1):77-85.
- [15] Teimuri-mofrad R, Hadi R, Tahmasebi B, Farhoudian S, Mehravar M, Nasiri R. Green synthesis of gold nanoparticles using plant extract: Mini-review. *Nanochemistry Research*. 2017;2(1):8-19.
16. Ravikumar S, Gokulakrishnan R, Boomi P. In vitro antibacterial activity of the metal oxide nanoparticles against urinary tract infectious bacterial pathogens. *Asian Pacific Journal of Tropical Disease*. 2012;2(2):85-9.
17. Taghavi Fardood S, Foroootan R, Moradnia F, Afshari Z, Ramazani A. Green synthesis, characterization, and photocatalytic activity of cobalt chromite spinel nanoparticles. *Materials Research Express*. 2020;7(1):015086.
18. Suresh D, Nethravathi PC, Udayabhanu, Rajanaika H, Nagabhushana H, Sharma SC. Green synthesis of multifunctional zinc oxide (ZnO) nanoparticles using Cassia fistula plant extract and their photodegradative, antioxidant and antibacterial activities. *Materials Science in Semiconductor Processing*. 2015;31:446-54.
19. Ramesh PS, Kokila T, Geetha D. Plant mediated green synthesis and antibacterial activity of silver nanoparticles using *Emblica officinalis* fruit extract. *Spectrochimica Acta Part A: Molecular and Biomolecular Spectroscopy*. 2015;142:339-43.
20. Atrak K, Ramazani A, Taghavi Fardood S. Eco-friendly synthesis of Mg_{0.5}Ni_{0.5}Al_xFe_{2-x}O₄ magnetic nanoparticles and study of their photocatalytic activity for degradation of direct blue 129 dye. *Journal of Photochemistry and Photobiology A: Chemistry*. 2019;382:111942.
21. Ahmed S, Ahmad M, Swami BL, Ikram S. A review on plants extract mediated synthesis of silver nanoparticles for antimicrobial applications: A green expertise. *Journal of Advanced Research*. 2016;7(1):17-28.
22. Taghavi Fardood S, Ramazani A, Asiabi PA, Joo SW. A Novel Green Synthesis of Copper Oxide Nanoparticles Using a Henna Extract Powder. *Journal of Structural Chemistry*. 2018;59(7):1737-43.
- [23] Taghavi Fardood S, Ramazani A. Black Tea Extract

- Mediated Green Synthesis of Copper Oxide Nanoparticles. Journal of Applied Chemical Research. 2018;12(2):8-15.
- [24] Taghavi Fardood S, Ramazani A, Joo SW. Sol-gel Synthesis and Characterization of Zinc Oxide Nanoparticles Using Black Tea Extract. Journal of Applied Chemical Research. 2017;11(4):8-17.
- [25] Taghavi Fardood S, Moradnia F, Mostafaei M, Afshari Z, Faramarzi V, Ganjkhanlu S. Biosynthesis of $MgFe_2O_4$ magnetic nanoparticles and its application in photodegradation of malachite green dye and kinetic study. Nanochemistry Research. 2019;4(1):86-93.
26. Eskandari Azar B, Ramazani A, Taghavi Fardood S, Morsali A. Green synthesis and characterization of $ZnAl_2O_4@ZnO$ nanocomposite and its environmental applications in rapid dye degradation. Optik. 2020;208:164129.
27. Moradnia F, Ramazani A, Fardood ST, Gouranlou F. A novel green synthesis and characterization of tetragonal-spinel $MgMn_2O_4$ nanoparticles by tragacanth gel and studies of its photocatalytic activity for degradation of reactive blue 21 dye under visible light. Materials Research Express. 2019;6(7):075057.
- [28] Taghavi Fardood S, Ramazani A, Moradnia F, Afshari Z, Ganjkhanlu S, Yekke Zare F. Green Synthesis of ZnO Nanoparticles via Sol-gel Method and Investigation of Its Application in Solvent-free Synthesis of 12-Aryltetrahydrobenzo[α]xanthene-11-one Derivatives Under Microwave Irradiation. Chemical Methodologies. 2019;3(6):696-706.
- [29] Nouri J, Khoshravesh T, Khanahmadzadeh S, Salehabadi A, Enhessari M. Synthesis, characterization and optical band gap of Lithium cathode materials: $Li_2Ni_8O_{10}$ and $LiMn_2O_4$ nanoparticles. International Journal of Nano Dimension. 2016;7(1):15-24.
30. Moradnia F, Taghavi Fardood S, Ramazani A, Gupta VK. Green synthesis of recyclable $MgFeCrO_4$ spinel nanoparticles for rapid photodegradation of direct black 122 dye. Journal of Photochemistry and Photobiology A: Chemistry. 2020;392:112433.